| OF |
AD
A067595

END
DATE
FILMED
6-79
DDC

REPORT DOCUMENTATION PAGE	READ INSTRUCTIONS BEFORE COMPLETING FORM

1. REPORT NUMBER	2. GOVT ACCESSION NO.	3. RECIPIENT'S CATALOG NUMBER
6079.32-MC and 12943.13-MS		

4. TITLE (and Subtitle)	5. TYPE OF REPORT & PERIOD COVERED
Properties of New Transition Metal Chalcogenides and Pnictides.	Final Report. 1 Feb 66 — 28 Feb 79,
	6. PERFORMING ORG. REPORT NUMBER

7. AUTHOR(s)	8. CONTRACT OR GRANT NUMBER(s)
Aaron/Wold	DA-31-124-ARO-D-433; DA-ARO-D-31-124-71-G78, 73-G18; DAAG29 76 G 0028; 78 G 0028

9. PERFORMING ORGANIZATION NAME AND ADDRESS	10. PROGRAM ELEMENT, PROJECT, TASK AREA & WORK UNIT NUMBERS
Brown University Providence, Rhode Island 02912	ARO, ARO

11. CONTROLLING OFFICE NAME AND ADDRESS	12. REPORT DATE
U. S. Army Research Office P. O. Box 12211 Research Triangle Park, NC 27709	Apr 1979
	13. NUMBER OF PAGES
	59

14. MONITORING AGENCY NAME & ADDRESS(if different from Controlling Office)	15. SECURITY CLASS. (of this report)
	Unclassified
	15a. DECLASSIFICATION/DOWNGRADING SCHEDULE

16. DISTRIBUTION STATEMENT (of this Report)

Approved for public release; distribution unlimited.

17. DISTRIBUTION STATEMENT (of the abstract entered in Block 20, if different from Report)

18. SUPPLEMENTARY NOTES

The view, opinions, and/or findings contained in this report are those of the author(s) and should not be construed as an official Department of the Army position, policy, or decision, unless so designated by other documentation.

19. KEY WORDS (Continue on reverse side if necessary and identify by block number)

magnetic compounds	phosphides
phase transformations	selenides
transition metals	high pressure phase transformations
semiconductors	

20. ABSTRACT (Continue on reverse side if necessary and identify by block number)

This report presents the results of studies of new transition metal magnetic compounds and includes (1) high pressure phase transformation studies of $Pd_{(1-x)}M_{(x)}Se_2$ (M=Ru, Co, Ni) and of $M_{(1-x)}Rh_{(x)}Se_2$ (M=Pd, Pt), (2) preparation and properties of indium antimony selenides, and (3) crystal growth and characterization of the transition metal phosphides CuP_2, NiP_2, and RhP_3.

DD FORM 1473 EDITION OF 1 NOV 65 IS OBSOLETE	Unclassified

The following manuscripts have been either submitted for publication or accepted for publication in various journals:

1. High Pressure Phase Transformation Studies of $Pd_{1-x}M_xSe_2$ (M=Ru,Co,Ni), D. Avignant, D. Carre, R. Collins, and A. Wold, Accepted for publication in Materials Research Bulletin.

2. High Pressure Phase Transformation Studies of $M_{1-x}Rh_xSe_2$ (M=Pd,Pt), D. Carre, D. Avignant, R. Collins, and A. Wold, Accepted for publication in Journal of Inorganic Chemistry.

3. Preparation and Properties of Two Indium Antimony Selenides, M. Spiesser, R. P. Gruska, S. N. Subbarao, C. A. Castro, and A. Wold, Journal of Solid State Chemistry, 26, 111-114 (1978).

4. Crystal Growth and Characterization of the Transition-Metal Phosphides CuP_2, NiP_2, and RhP_3, J. P. Odile, S. Soled, C. A. Castro, and A. Wold, Journal of Inorganic Chemistry, 17, 283 (1978).

79 04 16 053

HIGH PRESSURE PHASE TRANSFORMATION STUDIES OF $Pd_{1-x}M_xSe_2$ (M=Ru,Co,Ni)

D. Avignant, D. Carré, R. Collins, and A. Wold
Department of Chemistry, Brown University
Providence, Rhode Island 02912

ABSTRACT:

Members of the system $Pd_{1-x}M_xSe_2$ (M=Ru,Co,Ni), prepared at ambient pressure, consisted of mixtures of $PdSe_2$ and pyrite phases. Compositions with $x > 0.4$ for Ru and $x > 0.3$ for Co and Ni, prepared at a pressure of 50 Kbars and 1000°C, gave a single phase region crystallizing with the pyrite structure.

Introduction

$PdSe_2$ crystallizes with a layer structure (space group Pbca; a=5.741, b=5.866, c=7.691Å) Grønvold and Røst (1) have indicated that $PdSe_2$ may be described in terms of an elongated pyrite structure. At pressures as high as 65 Kbars, Bither (2) observed a compression in the interlayer direction but did not observe a transformation to a pyrite phase. He also noted that rhodium doped $PdSe_2$ did form a pyrite phase (a∿6.12Å) at high pressure. Carré, et al. (3) studied the system $Pd_{1-x}Rh_xSe_2$ (0.1 ≤ x ≤ 0.9) and reported that at 750°C and ambient pressure three structure types were obtained namely, $PdSe_2$, $RhSe_2$ ($IrSe_2$ structure) and $RhSe_2$ (pyrite structure). They also reported that when the composition $Pd_{0.8}Rh_{0.2}Se_2$ was heated at 1000°C and 50 Kbars, a mixture of an orthorhombic and pyrite phases were obtained. However, for x ≥ 0.3, a solid solution having the pyrite structure resulted.

The systems $Pd_{1-x}M_xSe_2$ (M=Co,Ni,Ru) were studied under conditions of ambient pressure as well as 50 Kbars to see the relative effect of

substitution of first and second row transition metals for Pd on the nature of high pressure phase transformation.

Experimental

Ambient Pressure Synthesis - Cobalt and nickel (99.99%) were reduced prior to use by heating nickel under a 15% hydrogen/85% argon mixture for 3 hours at 600°C and cobalt for 8 hours at 850°C. They were then subsequently heated under a dynamic vacuum at 200°C for several hours to insure the removal of any hydrogen formed during the reduction. The selenium, palladium and ruthenium (99.99%) were not purified further.

All polycrystalline samples were prepared by reacting stoichiometric quantities of the elements in evacuated silica tubes for one week at temperatures between 600°C and 750°C. Several intermittent grindings were carried out during the course of the preparations.

High Pressure Synthesis - The reacted polycrystalline samples were subjected to 50 Kbars pressure and temperatures ranging from 1000 to 1200°C for 1 1/2 hours. At the end of each experiment the temperature was lowered to room temperature over a period of twenty minutes and the pressure subsequently reduced to one atmosphere.

X-ray Analysis and Density Measurements - To determine the phases present in each sample, powder diffraction patterns were obtained with a Norelco diffractometer using CuKα radiation (λ=1.5405Å) and equipped with a graphite monochromator located in the diffracted beam. Precision lattice parameters were calculated from a least squares refinement of the observed versus the calculated $\sin^2\theta$ values corrected relative to a KCl standard. Densities were determined by the hydrostatic technique described by Adams (4) with

FIG. 1
Variation in cell edge with composition for the high pressure $Pd_{1-x}Ru_xSe_2$ cubic system.

FIG.2
Variation in cell edge with composition for the high pressure $Pd_{1-x}M_xSe_2$ (M=Co,Ni) cubic system.

perfluoro (1-methyldecalin) as the
density fluid and a high purity silicon
crystal (ρ=2.328 g/cc at 22°C) as the
standard.

Results and Discussion

Ambient Pressure - For the system
$Pd_{1-x}Ru_xSe_2$ (0.1 ≤ x ≤ 0.9) each
composition prepared at 700°C consisted
of a mixture containing $PdSe_2$ (orthor-
hombic structure) and $RuSe_2$ (pyrite
structure). Samples of the system
$Pd_{1-x}Ni_xSe_2$ (0.1 ≤ x ≤ 0.9) were
prepared at 650°C and on x-ray
analysis gave a mixture of $PdSe_2$ and
$NiSe_2$ (pyrite). Each member of the
system $Pd_{1-x}Co_xSe_2$ (0.1 ≤ x ≤ 0.9)
prepared at 750°C consisted of a mixture
of $PdSe_2$ and $CoSe_2$.

High Pressure - A single phase region,
with the pyrite structure, was found for
x ≥ 0.4 in the $Pd_{1-x}Ru_xSe_2$ system when
the samples were prepared at 1000°C and
50 Kbars. The lattice parameters and
densities of these compounds are listed
in Table I and Figure 1 shows the variation
of a_o as a function of composition.

When members of the systems $Pd_{1-x}M_xSe_2$
(M=Ni,Co) are subjected to 50 Kbars
pressure and 1000°C products which were
single phase with the pyrite structure
were obtained for x > 0.3. The lattice
constants and densities of these compounds
are given in Table II and Figure 2 shows
the variation of a_o as a function of the
composition.

The limited range of solid solution
formation in the systems $Pd_{1-x}M_xSe_2$
(M=Ru,Ni,Co) may be attributed to the
fundamental difference between the $PdSe_2$
and pyrite structures. $PdSe_2$ crystallizes
as a layer structure (space group Pbca)
which is shown in Figure 3. The structure
has been described as an elongated pyrite
which favors a square planar coordination
for the d^8 Pd. In contrast the pyrite
structure (Figure 4) is related to sodium
chloride with the cations occupying
octahedral sites. The packing of the

FIG. 3
The $PdSe_2$ Structure

FIG. 4
The Pyrite Structure

atoms is more efficient in the pyrite structure and hence the denser pyrite structure is favored at elevated pressure.

TABLE I

Lattice Constants and Densities for $Pd_{1-x}Ru_xSe_2$
Phases Obtained at 50 Kbars Pressure and 1000°C

Phase	a_o (Å)	ρ_{exp} (g/cm^3)	ρ_{calc} (g/cm^3)
$Pd_{0.6}Ru_{0.4}Se_2$	5.937	8.3(1)	8.33
$Pd_{0.4}Ru_{0.6}Se_2$	5.937	8.3(1)	8.30
$Pd_{0.2}Ru_{0.8}Se_2$	5.935	8.2(1)	8.27
$RuSe_2$	5.930	8.2(1)	8.25

TABLE II

Lattice Constants and Densities for $Pd_{1-x}M_xSe_2$ (M=Ni,Co)
Phases Obtained at 50 Kbars Pressure and 1000°C

| Phase	a_o (Å)	ρ_{exp} (g/cm^3)	ρ_{calc} (g/cm^3)
$Pd_{0.6}Ni_{0.4}Se_2$	6.102	7.1(1)	7.17
$Pd_{0.4}Ni_{0.6}Se_2$	6.058	7.0(1)	7.05
$Pd_{0.2}Ni_{0.8}Se_2$	5.991	6.9(1)	6.99
$NiSe_2$	5.959	6.7(1)	6.80
$Pd_{0.6}Co_{0.4}Se_2$	6.084	7.2(1)	7.24
$Pd_{0.4}Co_{0.6}Se_2$	5.975	7.3(1)	7.34
$Pd_{0.2}Co_{0.8}Se_2$	5.900	7.3(1)	7.32
$CoSe_2$	5.850	7.1(1)	7.19

Acknowledgement

References

1. F. Grønvold and E. Røst, Acta Cryst., <u>10</u>, 379 (1957).

2. T. Bither, private communication.

3. D. Carré, D. Avignant, R. Collins and A. Wold, J. Inorg. Chem., to be published.

4. R. A. Adams, Ph.D. Thesis, Brown University (1973).
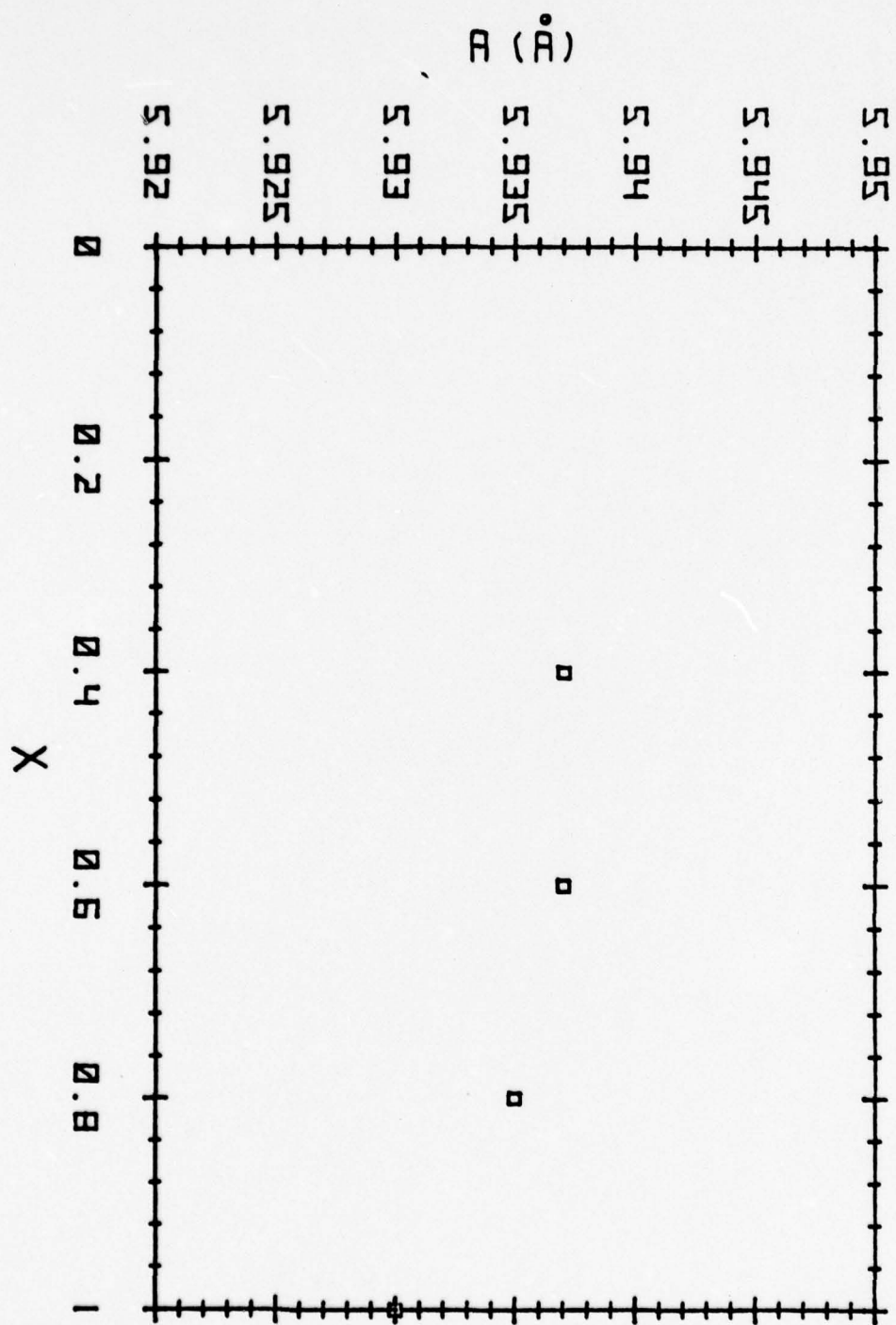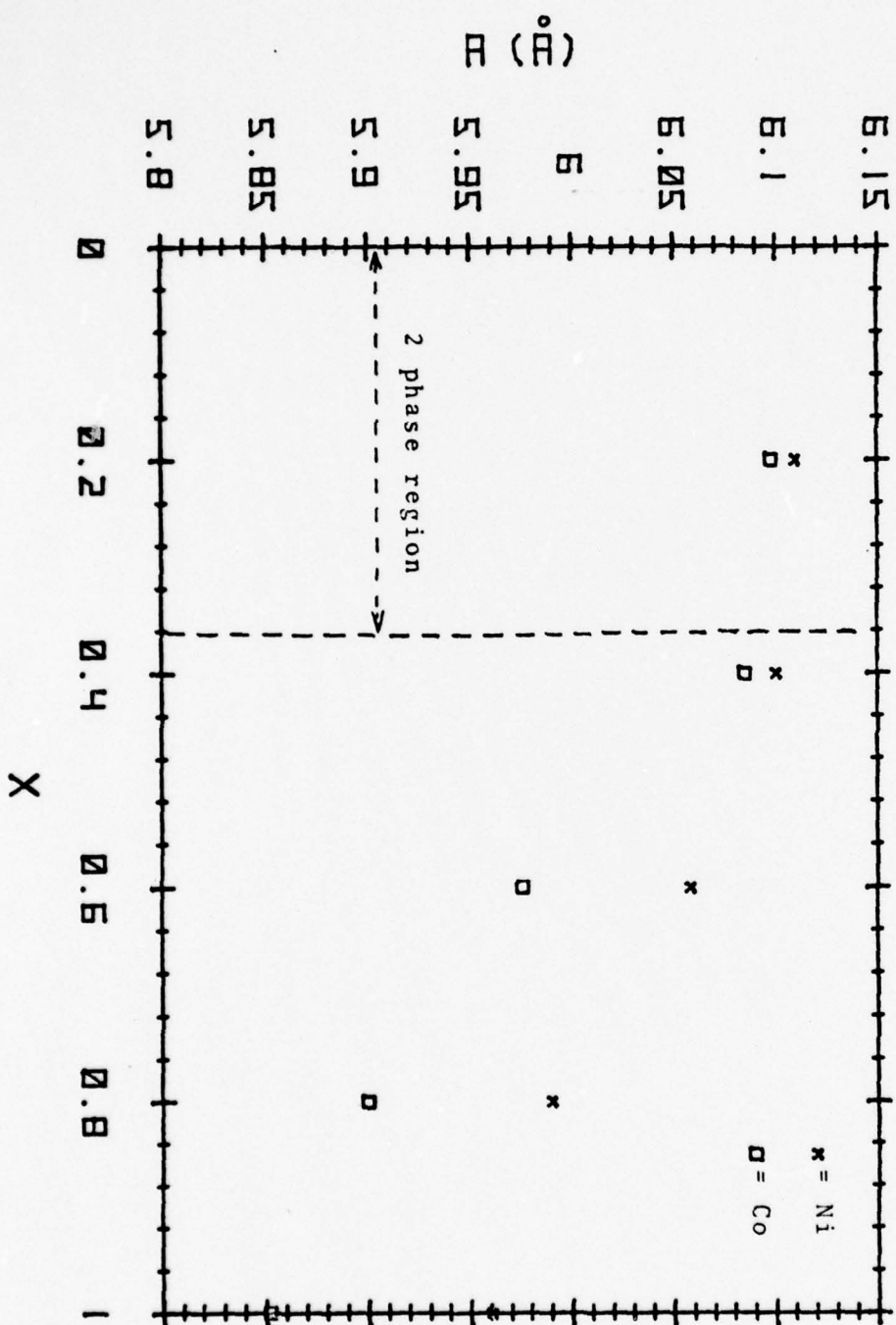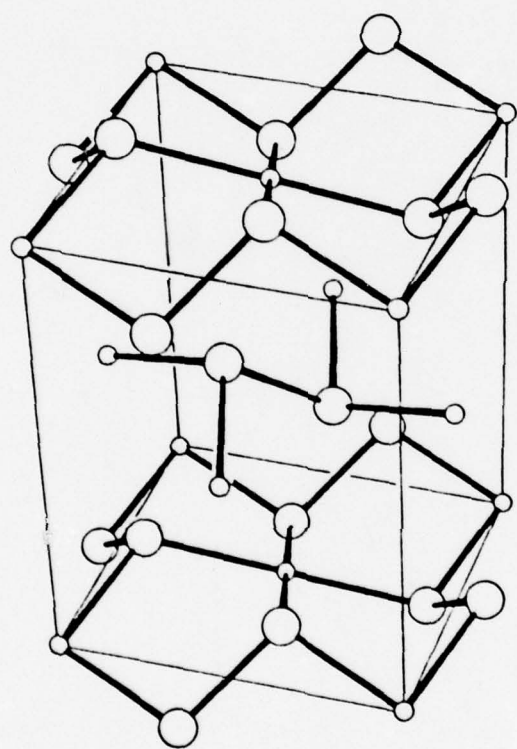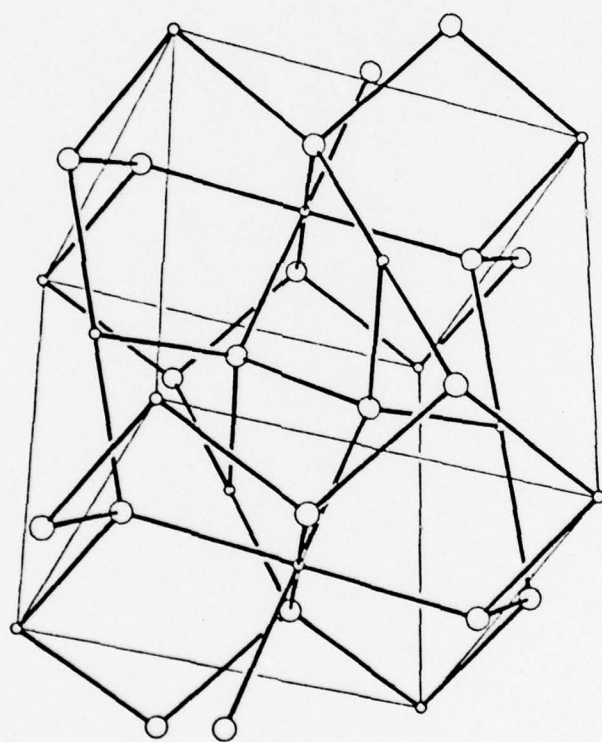
MANUSCRIPT #2

HIGH PRESSURE PHASE TRANSFORMATION STUDIES

OF $M_{1-x}Rh_xSe_2$ (M = Pd, Pt)

D. Carre

Universite Paris V
Faculte de Pharmacie
Laboratoire de Physique et de Chimie
4, Avenue de l'Observatoire
75006 Paris
FRANCE

D. Avignant

Universite de Clermont-Ferrand
Laboratoire de Chimie Des Solides
B.P. 45
63170 Aubiere
FRANCE

and

R. C. Collins and A. Wold[*]

Brown University
Department of Chemistry
Providence, Rhode Island 02912

[*]To whom all correspondence should be addressed.

ABSTRACT

Members of the system $Pd_{1-x}Rh_xSe_2$, prepared at ambient pressure, consisted of mixtures of $PdSe_2$ and $RhSe_2$. Compositions with $x \geq 0.3$, subjected to a pressure of 50 Kbars and 1000°C, gave a single phase region crystallizing with the pyrite structure. For the system $Pt_{1-x}Rh_xSe_2$ ($x \leq 0.4$) sample preparation at 1000°C and ambient pressure yielded a solid solution crystallizing with a CdI_2 structure. A high pressure phase transformation was not observed for this system at 50 Kbars pressure and 1000°C.

INTRODUCTION

A number of transition metal ditellurides may be induced to undergo a
high pressure phase transformation from a cadmium iodide structure to a
pyrite structure by chemical substitution. Among the systems which have
been studied are $Ni_{1-x}Fe_xTe_2$ (1) and $Pd_{1-x}Rh_xTe_2$(2). Although $NiTe_2$ under-
goes only a partial transformation from a cadmium iodide structure to a
pyrite structure at 89 Kbars (3), a single phase pyrite region may be
obtained for the system $Ni_{1-x}Fe_xTe_2$ ($0.4 \leq x \leq 0.8$) at 60 Kbars pressure (1).
$PdTe_2$ also crystallizes with the cadmium iodide structure at ambient pressure.
However, at 60 Kbars pressure a complete transformation to a pyrite phase
was obtained for $Pd_{1-x}Rh_xTe_2$ ($x \geq 0.6$) (2).

At ambient pressure $PdSe_2$ crystallizes with a layer structure (space group
Pbca; a = 5.741, b = 5.866, c = 7.691Å). Grønvold and Røst (4) have indicated
that $PdSe_2$ may be described in terms of an elongated pyrite structure. At
pressures as high as 65 Kbars, Bither (5) observed only a compression of
the structure in the interlayer direction but he did not report a transformation
to the pyrite structure. He also noted that high pressure synthesis of
rhodium substituted $PdSe_2$ yielded a mixture containing a $PdSe_2$ high pressure
orthorhombic phase and a pyrite phase (a ∿ 6.12Å). $RhSe_2$ has been reported
to adopt either an orthorhombic $IrSe_2$ structure (6) (Pnam with a = 20.91,
b = 5.951, c = 3.709Å) at room temperature or a pyrite structure (a ∿ 6.01Å
extrapolated value) at high temperature (7). Comparison of the cell constants
for these two pyrite phases indicates that the pyrite phase obtained by Bither (5)
for rhodium substituted $PdSe_2$ contains rhodium.

$PtSe_2$ crystallizes with the CdI_2 structure (space group $P\bar{3}m1$; a = 3.724, c = 5.062). High pressure phase transformations for $PtSe_2$ have not been reported.

The systems $M_{1-x}Rh_xSe_2$ (M = Pd, Pt) were investigated at both ambient pressure and under high pressure in order to determine the extent of solid solution and the effect of the rhodium substitution for palladium and platinum on the existence of high pressure phases.

EXPERIMENTAL

All polycrystalline samples were prepared by reacting stoichiometric quantities of the elements in evacuated silica tubes. The samples were heated for one week with several intermittent grindings. At the end of each heat treatment the samples were cooled to room temperature at the rate of 100°C/hour.

The reacted polycrystalline samples were subjected to 1000°C and 50 Kbars pressure for 1 1/2 hours in a belt apparatus described by Hall (8). Reactions were not carried out at higher temperatures in order to avoid decomposition of the products. At the end of each experiment, the sample was allowed to cool for fifteen minutes and the pressure was then reduced to one atmosphere (ambient pressure).

The phases present in each sample were identified from powder patterns obtained with a Norelco diffractometer equipped with a high intensity copper source and a graphite monochromater (CuKα = 1.5418Å) located in the diffracted beam. Lattice parameters were calculated from a least-squares refinement using 2θ angles corrected relative to a KCl internal standard. Densities were measured by the hydrostatic technique described by Adams (9). Perfluoro (1-methyldecalin) served as the density fluid which was calibrated with a high purity silicon crystal (ρ = 2.33 g/cm^3 at 25°C).

RESULTS

Ambient Pressure - For the system $Pd_{1-x}Rh_xSe_2$ ($0.1 \leq x \leq 0.9$) the products obtained at 750°C and ambient pressure contained three structure types, namely, $PdSe_2$, $RhSe_2$ ($IrSe_2$ structure) and $RhSe_2$ (pyrite structure).

For the system $Pt_{1-x}Rh_xSe_2$ ($x \leq 0.4$) sample preparation at 1000°C yielded a single phase region with the CdI_2 structure. Cell constants are plotted as a function of composition in Figure 1. In addition to this solid solution a $RhSe_2$ pyrite phase appeared for compositions where x is somewhat greater than 0.4.

High Pressure - When subjected to 50 Kbars pressure and 1000°C, $PdSe_2$ retained an orthorhombic structure with a = 5.758, b = 5.858 and c = 7.628Å. The cell volume 257.3Å^3 for this product is smaller than 259.0Å^3 reported by Grønvold and Røst for $PdSe_2$ prepared at ambient pressure. For the composition $Pd_{0.8}Rh_{0.2}Se_2$, a mixture of the orthorhombic and pyrite phases were obtained. However, for $x \geq 0.3$ a solid solution resulted with the pyrite structure. Lattice constants and densities are listed in Table I. The lattice constants are plotted as a function of composition in Figure 2. For the system $Pt_{1-x}Rh_xSe_2$, all samples subjected to high pressure consisted of two phases: $PtSe_2$ (CdI_2 structure) and $RhSe_2$ (pyrite structure).

DISCUSSION

$PdSe_2$ has a layer structure (Figure 3) which can be derived from an elongation of the anion octahedra of the pyrite structure (Figure 4). This elongation generates square planar coordination for the $4d^8$ Pd. In both structures anions are found as Se_2^{-2} pairs. In the CdI_2 structure (Figure 5) in which the platinum dichalcogenides crystallize, the $5d^6$ Pt species occupy octahedral sites between alternate anion layers.

Transformations from the $PdSe_2$ and CdI_2 structures to the more dense pyrite structure are favored by high pressure. Although such a phase transformation was not observed at 50 Kbars pressure for $PdSe_2$, chemical substitution of rhodium for palladium did induce a transformation to the pyrite structure. For such a transformation there is no change in the electronic structure of Pd since (d^8) Pd is present in both phases. For $PtSe_2$ a phase transformation could not be promoted via rhodium chemical substitution under the same experimental conditions used for the transformation of a Rh substituted $PdSe_2$.

In Table II structure types and known phase transformations to the pyrite structure are given for the Ni, Pd, and Pt dichalcogenides with chemical substitutions. A pyrite phase is listed for each of the Ni dichalcogenides and for $PdSe_2$ and $PdTe_2$. Chemical substitution should promote a phase transformation to the pyrite structure for PdS_2 as observed here for $PdSe_2$. Phase transformations for the Pt dichalcogenides have not been reported. Indeed, attempts to induce a transformation for $PtSe_2$ with rhodium chemical substitution at 50 Kbars pressure were unsuccessful. Comparison of the solid state chemistry of Ni, Pd, and Pt, indicates that $5d^8$ Pt cannot occupy an octahedral site, whereas d^8 Ni and d^8 Pd are known to occupy octahedral sites. This is consistent with the failure to observe a phase transition for rhodium-substituted platinum diselenide.

ACKNOWLEDGEMENTS

REFERENCES

1. R. Korenstein, R. L. Henry, and A. Wold, Inorg. Chem., 15, 33031 (1976).

2. E. McCarron, R. Korenstein, and A. Wold, Mat. Res. Bull., 11, 1457 (1976).

3. T. A. Bither, R. J. Bouchard, W. H. Cloud, P. C. Donohue, and W. J. Siemons, Inorg. Chem., 7, 2208 (1968).

4. F. Grønvold and E. Røst, Acta. Cryst., 10, 329 (1957).

5. T. Bither, Private Communication.

6. F. Hulliger, Nature, 204, 644 (1964).

7. T. E. Rummery and R. D. Heyding, Can. J. Chem., 45, 131 (1967).

8. H. T. Hall, Rev. Sci. Instrum., 31, 25 (1960).

9. R. A. Adams, Ph.D. Thesis, Brown University (1973).

10. F. Hulliger, "Structure and Bonding", Vol. 4, Springer-Verlag, New York, (1968).

TABLE I

Lattice Constants and Densities for $Pd_{1-x}Rh_xSe_2$ Phases Obtained at 50 Kbars Pressure and 1000°C

Phase	a_o(Å)	ρ_{exp}(g/cm^3)	ρ_{calc}(g/cm^3)
$Pd_{0.7}Rh_{0.3}Se_2$	6.123(2)	7.5(1)	7.62
$Pd_{0.6}Rh_{0.4}Se_2$	6.109(2)	7.6(1)	7.66
$Pd_{0.4}Rh_{0.6}Se_2$	6.076(2)	7.7(1)	7.76
$Pd_{0.2}Rh_{0.8}Se_2$	6.048(2)	7.8(1)	7.85
$RhSe_2$	6.018(2)	7.9(1)	7.95

TABLE II

Structure Types for Ni, Pd, and Pt

Dichalcogenides. P = pyrite. An arrow indicates a reported high pressure phase transformation to the pyrite structure with chemical substitution.

Metal/Chalcogenide

	S	Se	Te
Ni	P	P	CdI_2[*] → P
Pd	$PdSe_2$	$PdSe_2$ → P	CdI_2[**] → P
Pt	CdI_2	CdI_2	CdI_2

[*] System $Ni_{1-x}Fe_xTe_2$

[**] System $Pd_{1-x}Rh_xTe_2$

References: NiS_2, $NiSe_2$, and PtX_2 (x = S, Se, Te)[10]
$NiTe_2$[1]
$PdSe_2$, this work, $PdTe_2$[3]

FIGURE CAPTION SHEET

FIGURE 1   -   Variation in cell edge with composition for the ambient
pressure $Pt_{1-x}Rh_xSe_2$ hexagonal system.

FIGURE 2   -   Variation in cell edge with composition for the high pressure
$Pd_{1-x}Rh_xSe_2$ cubic system.

FIGURE 3   -   The $PdSe_2$ structure.

FIGURE 4   -   The Pyrite structure.

FIGURE 5   -   The CdI_2 structure.

FIG 1

FIG. 2

FIG. 3

FIG 4

FIG 5
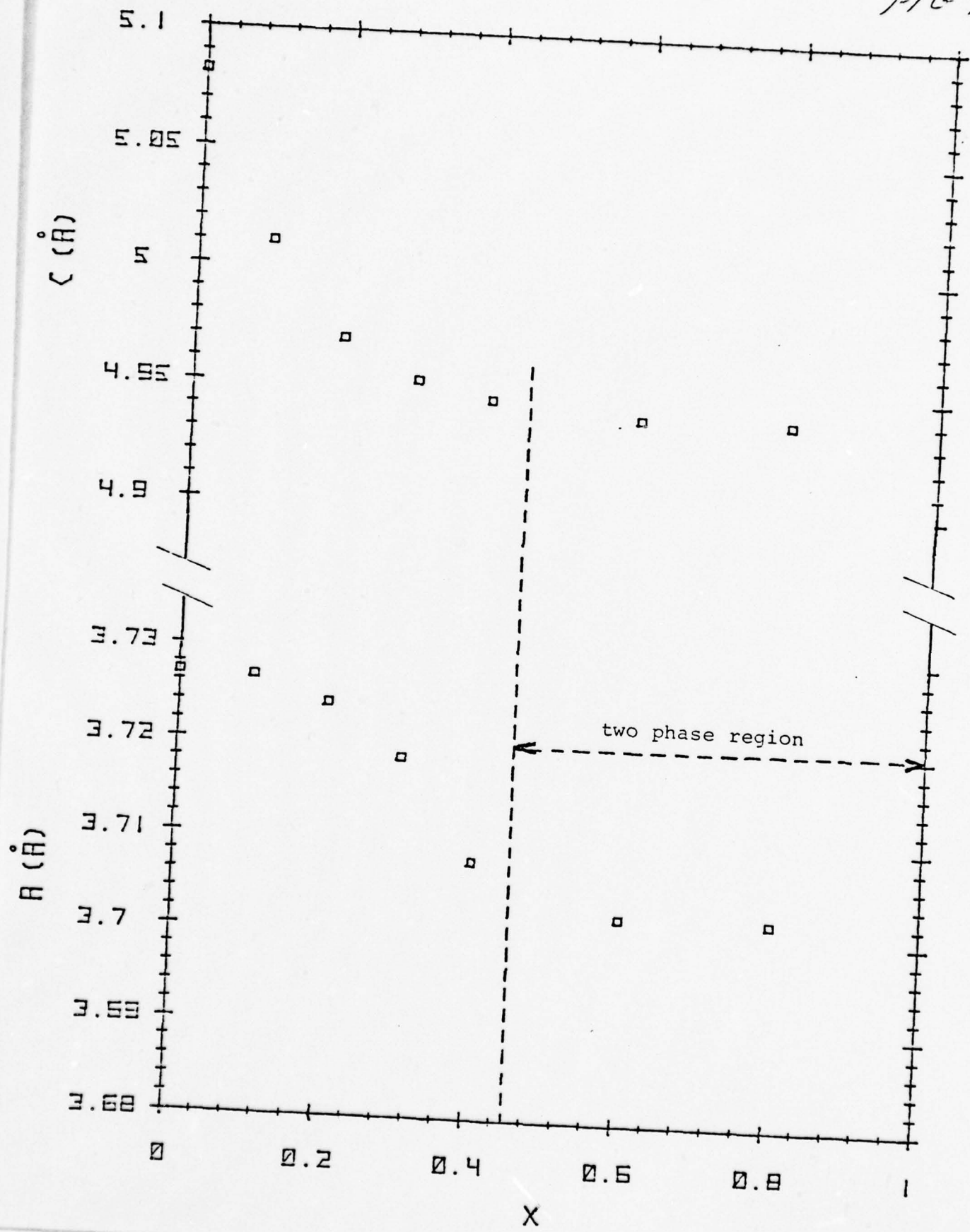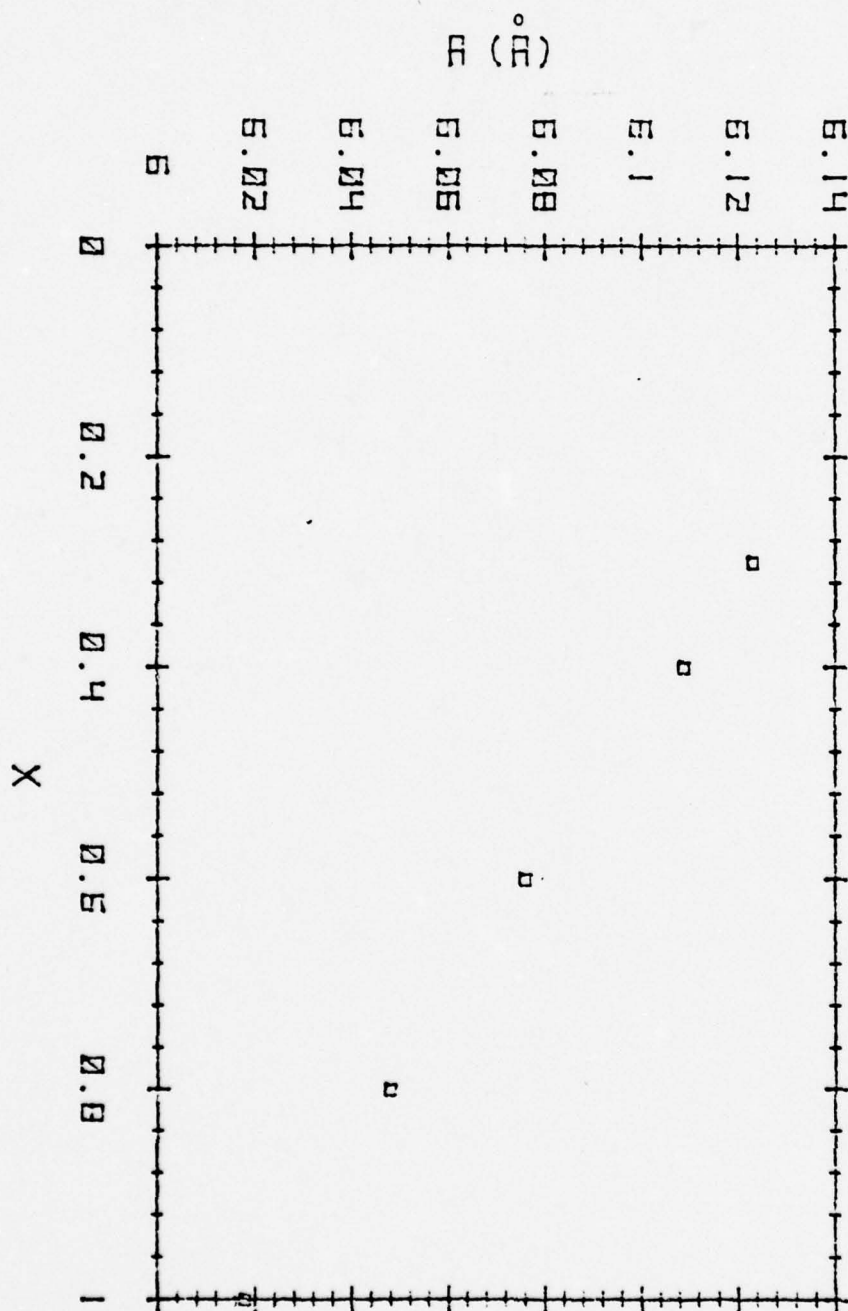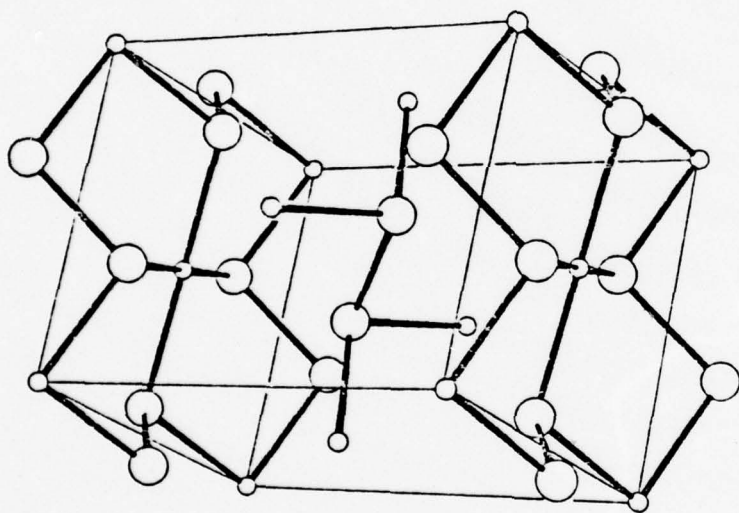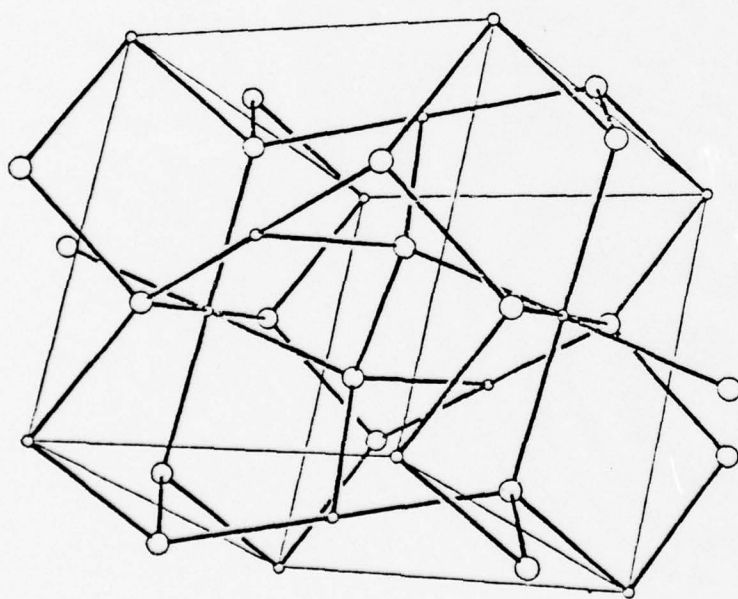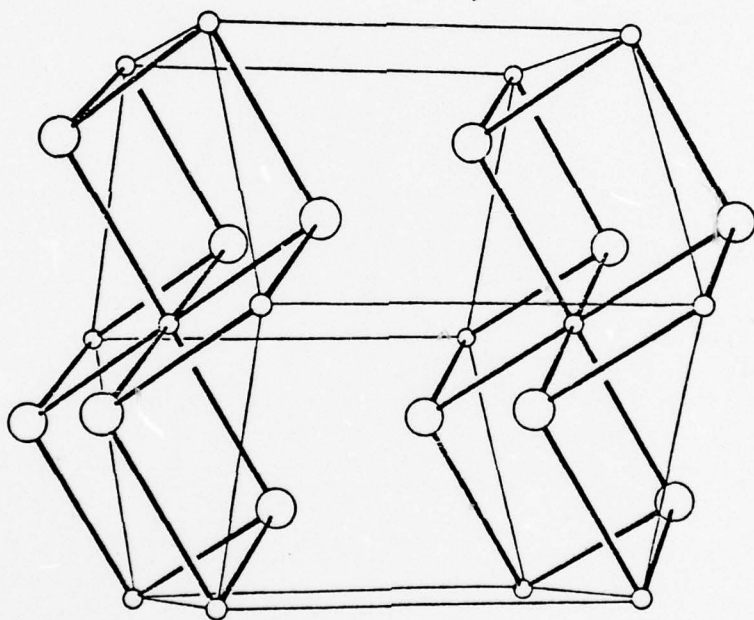
MANUSCRIPT #3

PREPARATION AND PROPERTIES OF TWO INDIUM ANTIMONY SELENIDES

Michel Spiesser

Laboratoire de Chimie Minerale A, U.E.R. de Chimie de Nantes,
Nantes, France

and

Robert P. Gruska, S. N. Subbarao, Carlos A. Castro, and Aaron Wold*
Department of Chemistry, Brown University
Providence, Rhode Island   02912

*To whom all correspondence should be addressed.

ABSTRACT

Crystals of antimony-doped In_2Se_3 were grown by the Bridgman method. This compound, whose composition is $In_{1.8}Sb_{0.2}Se_3$, appears to be isostructural with $In_{1.9}As_{0.1}Se_3$. The refined unit cell parameters are $\underline{a}$ = 3.97(1), $\underline{c}$ = 18.87(1)$\overset{o}{A}$. Orthorhombic crystals of $InSbSe_3$ were grown from an isothermal melt. The refined unit cell parameters are $\underline{a}$ = 9.43(1), $\underline{b}$ = 14.02(5), and $\underline{c}$ = 3.96(1)$\overset{o}{A}$. These parameters agree with those determined for α-$InSbSe_3$ by other studies. The observed densities measured by a hydrostatic technique are 5.98(3) gm/cm^3 for $In_{1.8}Sb_{0.2}Se_3$ and 6.07(2) gm/cm^3 for $InSbSe_3$. The room temperature d.c. resistivity for $In_{1.8}Sb_{0.2}Se_3$ has been found to be 4.4×10^4 Ω-cm, whereas that of $InSbSe_3$ has been found to be 15.2(1) Ω-cm. A resistivity versus temperature study has been carried out for $InSbSe_3$ between 230°-400°K. Optical studies indicate that $In_{1.8}Sb_{0.2}Se_3$ is an n-type semiconductor with a band gap of 1.1 eV and $InSbSe_3$ is a p-type semiconductor with a band gap of 0.92 eV.

INTRODUCTION

A high temperature phase of indium (III) sulfide has been stabilized at room temperature by doping with arsenic or antimony (1,2). The resulting n-type semiconductors have the stoichiometry $In_{1.9}As_{0.1}S_3$ and $In_{1.8}Sb_{0.2}S_3$. Crystals of an analogous arsenic-doped indium (III) selenide, $In_{1.9}As_{0.1}Se_3$, have recently been grown in this laboratory (3). This compound is structurally related to the doped indium sulfide; however, there is a doubling of the c axis in the selenide. The compound $In_{1.9}As_{0.1}Se_3$ is hexagonal and the sulfides $In_{1.9}As_{0.1}S_3$ and $In_{1.8}Sb_{0.2}S_3$, are trigonal.

This work reports the synthesis and characterization of an antimony-doped indium selenide, $In_{1.8}Sb_{0.2}Se_3$. An impurity encountered in the initial synthesis of this phase was identified as $InSbSe_3$. The preparation and characterization of $InSbSe_3$ is also reported here.

EXPERIMENTAL

Single-phase crystals of $In_{1.8}Sb_{0.2}Se_3$ were grown by the Bridgman method. Indium (J. Matthey and Co., 99.999%) was purified by zone melting under vacuum prior to use. Antimony (Gallard-Schlesinger, 99.999%) and Selenium (Leico, 99.999%) were used without further purification. A sealed, evacuated silica tube containing the elements in correct stoichiometric amounts was placed in an isothermal furnace at 860°C for two days to insure a homogeneous melt. The sample was slow-cooled, then crushed, and placed in a tube designed (5) to facilitate the growth of a single crystal during the Bridgman process. The sample was suspended within the growth furnace (Hevi-Duty MK-2012) by means of silica hooks and kept at a

temperature of 880°C for one day. It was then lowered at a rate of 7.2 cm/day (see Fig. 1 for the furnace profile) for another three days after which the furnace was shut off and allowed to cool to room temperature. This process resulted in either a single crystal or several large grains which could be visually separated into single crystals.

Single crystals of $InSbSe_3$ were grown from the melt in an isothermal furnace. A sealed, evacuated 9 mm I.D. silica tube, containing the elements in stoichiometric amounts totaling three grams, was placed within an alundum core which had both ends closed with refractory wool. The core and tube were then heated to 825°C for five days, and allowed to slow cool. The product contained a number of grains which could be visually separated into single crystals.

X-RAY ANALYSIS

The samples prepared by the above procedures have been analyzed by X-ray diffraction of ground single crystals. A Norelco diffractometer with monochromatic radiation and a high density copper source was used $[\lambda(CuK\alpha_1) =$ 1.5405 Å]. Fast scans were obtained at a speed of 60°/hour in 2θ, whereas slow scans were made at a speed of 15°/Hour. Precision lattice parameters were calculated from a least-squares refinement of observed versus calculated values of $\sin^2\theta$ using silicon as the internal standard ($a_o = 5.430(1)$).

Density measurements of single crystals were made by a hydrostatic technique (6) using perfluoro (1-methyldecalin) as the liquid. In both cases, the liquid was first calibrated using a high purity silicon crystal

with its density taken as 2.328 gm/cm^3. All measurements were carried out at 25° ± 2°C.

ELECTRICAL MEASUREMENTS

The d.c. resistivities of single crystals of both compounds were obtained by the van der Pauw technique (7) utilizing a Hewlett-Packard 3450A voltmeter and a PAR TC-100.2AR constant-current supply. Indium alloy (Indalloy Solder #2) electrical contacts were applied to the crystal with an ultrasonic soldering device (Sonobond Corp. 12 Watt generator).

OPTICAL MEASUREMENTS

Optical absorption measurements were performed on thin crystals of both compounds at room temperature using a Cary 17 spectrophotometer operating in the absorbance mode.

RESULTS AND DISCUSSION

The compound $In_{1.8}Sb_{0.2}Se_3$ is isostructural with $In_{1.9}As_{0.1}Se_3$ (3). The system is hexagonal; the possible space groups are $P6_3mc$, $P\bar{6}2c$, and $P6_3/mmc$. The refined unit cell parameters for $In_{1.8}Sb_{0.2}Se_3$ are $\underline{a}$ = 3.97(1), $\underline{c}$ = 18.87(1)Å. Both these compounds appear to be closely related to the α-hexagonal phase of In_2Se_3 by Popovic, et al. (8). They reported two forms of $\alpha-In_2Se_3$, one hexagonal and the other rhombohedral. The first was obtained slow cooling in an isothermal furnace, the second was obtained by slow cooling in a furnace with a temperature gradient. Doping with

antimony apparently allows only the hexagonal form to crystallize, regardless of the cooling technique used. X-ray diffraction patterns of both $In_{1.8}Sb_{0.2}Se_3$ and the hexagonal form of α-In_2Se_3 give the same diffuseness of peaks (except for the 00ℓ reflections).

The preparation of single crystals of $In_{1.8}Sb_{0.2}Se_3$ was initially attempted by chemical vapor transport from the elements using chlorine as the transport agent. Pure, single phase crystals could not be grown by this technique, however. X-ray diffraction patterns of the ground products showed the presence of two impurity phases, one of which could be eliminated by quenching the samples in water. The impurity phase remaining corresponded to the compound identified as $InSbSe_3$ by Guliev, et al. (4).

All peaks on the X-ray diffraction patterns of $InSbSe_3$ samples prepared from the melt could be indexed using the refined unit cell parameters $\underline{a}$ = 9.43(1), $\underline{b}$ = 14.02(5), $\underline{c}$ = 3.96 (1)$\overset{o}{A}$. These parameters agree with the orthorhombic unit cell reported for $InSbSe_3$ by Guliev, et al. (4). This is a distorted hexagonal cell, with the translational periodicity in the a_o direction being half the translational periodicity of $In_{1.8}Sb_{0.2}Se_3$ in the c_o direction.

Crystals of $In_{1.8}Sb_{0.2}Se_3$ and $InSbSe_3$ were analyzed for antimony content (atomic absorption) by Jarrell-Ash Co. (Waltham, Mass.). The results are shown in Table I. Included in the table are the observed and calculated densities for both compounds.

The room temperature resistivity of $In_{1.8}Sb_{0.2}Se_3$ was found to be 4.4×10^4 Ω-cm. Because of its high resistivity, a temperature dependence study was not undertaken. The sign of the Seebeck coefficient showed it

to be an n-type semiconductor, as were $In_{1.9}As_{0.1}Se_3$ (3), $In_{1.9}As_{0.1}S_3$, and $In_{1.8}Sb_{0.2}S_3$(1).

Figure 2 is a plot of ρ versus 1000/T over the temperature range 230°-400°K for $InSbSe_3$. The line shown on the plot was fitted to the experimental data by the method of least-squares and yields a standard error of 0.5%. The activation energy calculated from its slope was found to be 0.047 eV. This low value suggests that the resistivity measurements were made in the extrinsic region of this compound. The sign of the Seebeck coefficient showed $InSbSe_3$ to be a p-type semiconductor.

The optical absorption spectra for $In_{1.8}Sb_{0.2}Se_3$ and $InSbSe_3$ are shown in Figures 3 and 4, respectively. The optical absorption edge occurs at approximately 1.1 eV for $In_{1.8}Sb_{0.2}Se_3$, as compared with 1.4 eV for $In_{1.9}As_{0.1}Se_3$ (3). The optical absorption edge for $InSbSe_3$ occurs at 0.92 eV.

ACKNOWLEDGEMENTS

REFERENCES

1. R. Diehl and R. Nitsche, J. Cryst. Growth, 20, 38 (1973).

2. R. Diehl, C. Carpentier, and R. Nitsche, Acta Cryst., B32, 1257 (1976).

3. A. Katty, C. A. Castro, J. P. Odile, S. Soled, and A. Wold, To appear in the J. of Solid State Chem.

4. T. N. Guliev, E. V. Magerramov, and P. G. Rustamov, Izv. Akad. Nauk. S.S.S.R., Neorg. Mater., $\underline{13}$(4), 627 (1977).

5. A. Lyons, D. Schleich, and A. Wold, Mat. Res. Bull., $\underline{11}$, 1155 (1976).

6. L. J. Cabri, Amer. Mineralog., $\underline{54}$, 539 (1969).

7. L. J. van der Pauw, Phillips Res. Rept., $\underline{16}$, 187 (1961).

8. S. Popovic, B. Celustka, and D. Bidjin, Phys. Stat. Sol. (a) $\underline{6}$, 301 (1971).

TABLE I

DENSITIES AND ANTIMONY PERCENTAGES BY WEIGHT

Compound	Observed Density (gm/cm^3)	Calculated Density (gm/cm^3)	Observed Percentage by Weight Antimony	Theoretical Percentage by Weight Antimony
$In_{1.8}Sb_{0.2}Se_3$	5.98 (3)	6.02	5.0 (1)	5.5
$InSbSe_3$	6.07(2)	6.11	22.8 (1)	23.7

MANUSCRIPT #4

CRYSTAL GROWTH AND CHARACTERIZATION OF THE TRANSITION METAL PHOSPHIDES

CuP_2, NiP_2 and RhP_3

J. P. Odile, S. Soled, C. A. Castro, and A. Wold

Department of Chemistry and Division of Engineering, Brown University, Providence, Rhode Island 02912.

ABSTRACT

Single crystals of the transition metal phosphide CuP_2, NiP_2 and RhP_3 were grown from a tin flux and, for the first time, their physical properties have been well characterized. In addition, single crystals of CuP_2 were grown by the chemical vapor transport technique, using chlorine as a transport agent. All three phosphides crystallize with structures having groups of anions bonded to one another. Although a tin content of 0.6 weight % was measured by atomic absorption in the flux grown CuP_2 crystals, the magnetic, electrical and optical properties of the flux and transported single crystals were very similar. From this study, CuP_2 was ascertained to be a diamagnetic p-type semiconductor with a band gap of 1.53 eV and NiP_2 a diamagnetic n-type semiconductor with a band gap of 0.73 eV. P-type metallic conduction and diamagnetic behavior were observed for RhP_3.

INTRODUCTION

Most of the early investigations of transition metal phosphides have focused on metal rich phases. The study of the phosphorus rich transition metal phosphides has been complicated by the formation of multiple phases during synthesis via direct combination of the elements and by difficulties in crystal growth (1,2). However, a recent interest in the semiconducting properties of these phases has prompted a more systematic study. Investigators from this laboratory have grown crystals of platinum diphosphide from a tin flux (3) and cobalt triphosphide using the chemical vapor transport technique (4). These techniques were used in the present work to prepare single crystals of the phosphorus rich transition metal phosphides CuP_2, NiP_2 and RhP_3.

These phosphides feature different types of anion arrangements. In the CuP_2 structure, the anion framework is comprised of edge sharing ten-membered puckered rings of phosphorus atoms lying approximately parallel to (100), that is, in a direction perpendicular to the plane of projection shown in Figure 1. Discrete pairs of copper atoms bridge these rings.

In NiP_2, the phosphorus atoms form square rings slightly tilted from the $(10\bar{1})$ plane as shown in Figure 2 with nickel atoms situated in the center of the rings. Short P-P bonds connect the atoms in adjacent planes.

RhP_3 adopts the skutterudite (5) structure. The phosphorus atoms cluster into planar four-membered rectangular rings, as illustrated in Figure 3. The cations are octahedrally coordinated by the anions whereas each anion is coordinated by two metal atoms and two other anions in a distorted tetrahedron. The unit cell is cubic and contains eight RhP_3 units.

Large (approximate average dimensions: 2x2x0.5 mm) and well characterized single crystals have been grown in order to determine the exact physical properties of these phases.

EXPERIMENTAL

1) <u>Chemical Vapor Transport</u>

Both copper (Johnson-Matthey, 99.999%) and nickel (Gallard-Schlessinger, 99.999%) were reduced in a dry 15% H_2/85% Ar atmosphere for four hours at 600°C to remove oxygen impurities. Rhodium (Engelhard, 99.99%), red phosphorus (Leico Industries, 5-9's) and chlorine (Linde, 99%) were used as supplied.

In order to prepare single crystals of CuP_2, stoichiometric amounts of the starting materials were introduced into silica tubes (28 cm x 13 mm) which were then evacuated to less than 2 torr. After the tubes were filled to a pressure of 50 torr of chlorine, they were sealed and placed in a transport furnace. A temperature profile was maintained for one day with the growth zone at 835°C and the charge zone at 815°C to remove any potential nucleation sites from the growth zone. After thermal equilibrium was established along the tube, the charge zone was set at 810°C and the growth zone cooled over a period of four days to a final temperature of 760°C. This gradient was maintained for 3-5 days, then the furnace was shut and allowed to cool to room temperature. Large black, shiny crystals of CuP_2 were obtained by this method. Similar attempts to grow crystals of NiP_2 and RhP_3 were unsuccessful.

2) Growth from a tin flux

Single crystals of CuP_2, NiP_2 and RhP_3 were grown from a tin flux (6).
The tin metal (99.5%) was purified by melting under a dynamic vacuum.
Stoichiometric amounts of the transition metal (Cu, Ni or Rh) and phosphorus
were placed in a silica tube and tin was added such that the resulting
mixture was at least eighty-five percent tin (by weight). The exact molar
ratios are listed in Table I. The tube was then evacuated to 2 torr,
sealed, and heated in a furnace at 35°C/hr to 1150°C. After a soaking
period of 12-15 hours at this temperature, the furnace was cooled at a constant
rate of 5°C/hr to 550°C. The tube was then removed from the furnace,
allowed to cool to room temperature and opened. Crystals were retrieved
by leaching away the solidified flux with hot dilute HCl. The crystals
of each phase were black, weighing up to 200 mg. Attempts to grow compositions
with a higher phosphorus content resulted in the formation of the already
reported phase Cu_4SnP_{10} in the Cu-P system (7). In the Ni-P and Rh-P
systems, NiP_2 and RhP_3 were the only phosphorus rich phases found.

3) Chemical Analysis

NiP_2 was analyzed for nickel using the photometric dimethylglyoxime
method (8). After 115 mg of crystals were dissolved in boiling aqua regia,
the solution was diluted to 250 ml with distilled water. To 1 ml of this
solution were added 1 ml of saturated bromine water, 4 ml of concentrated
NH_4OH, 35 ml of ethanol and 20 ml of a solution of dimethylglyoxime and
ethanol (0.2 g of DMG in 20 ml of EtOH). The resulting solution was diluted

to 100 ml with distilled water. The absorbance of the brownish nickel - DMG complex was measured at 540 nm using a Cary 14 spectrophotometer. The results were compared with standard nickel solutions made up by dissolving freshly reduced nickel powder in concentrated HCl. The standards obeyed Beer's law in the concentration range 1-3 μg Ni/ml. From the standard plot, an experimental weight percent of nickel of 49(1)% was calculated and found to be in good agreement with the theoretical value of 48.7% in NiP_2.

In order to check for flux contamination, single crystals of flux grown CuP_2 and NiP_2 were analyzed for tin content by atomic absorption by the Jarrell-Ash Division (Waltham, Mass.). Weight percents of tin of 0.6% and 1.2% were found for CuP_2 and NiP_2, respectively.

RESULTS

1) X-ray and Density Measurements

Powder diffraction patterns of ground single crystals of the different samples were obtained with a Norelco diffractometer using monochromatic radiation from a high intensity copper source ($\lambda_{CuK\alpha_1}$ = 1.5405Å). Cell parameters were determined from slow-scan (1/4°/minute) diffraction patterns over the range $12° \leq 2\theta \leq 130°$ with pure powdered silicon (Gallard-Schlesinger, 99.9999%) as an internal standard. The reflections were indexed on unit cells determined from single crystal studies of previous investigations (9, 10,11) and the precise lattice parameters were obtained using a least squares refinement from these reflections. The crystallographic data are listed in Table II.

The densities were determined using the hydrostatic technique (12). Perfluoro (1-methyldecalin) was used as a liquid and its density calibrated before each measurement with a silicon crystal (d = 2.328 g-cm^{-3} at 22°C). The good agreement between the experimental densities and the densities calculated from the cell parameters confirmed the stoichiometry of the phases.

2) Magnetic, Optical, and Electrical Measurements

Magnetic measurements were performed using the Faraday balance previously described by Morris and Wold (13). The magnetic susceptibilities were measured as a function of temperature from 77°K to 300°K at a field strength of 10.3 KOe. The molar susceptibilities of CuP_2 grown by chemical vapor transport (χ_M = -42.6 emu), and of CuP_2 (χ_M = -44.2 emu), NiP_2 (χ_M = - 19.0 emu), and RhP_3 (χ_M = -33.6 emu) all grown from a tin flux are negative and temperature independent thus indicating diamagnetic behavior. No corrections were made for the core diamagnetism of these samples because of the large uncertainty in the magnitude of the corrections compared to the magnitude of the values of the measured susceptibilities. The absence of ferromagnetic impurities in the crystals investigated was ascertained by the lack of field dependence of the susceptibility.

Optical measurements on polished single crystals were performed at room temperature on a Cary 17 dual beam scanning spectrophotometer operating in the absorbance mode over the range 25000 Å - 3500 Å. From these measurements, the values of the optical band gaps were found to be Eg = 1.55(5) eV for CuP_2 grown by chemical vapor transport, Eg = 1.51(5) eV for CuP_2 grown from a tin flux and Eg = 0.73(5) eV for NiP_2 (Figure 4). An absorption

edge was not detected for RhP_3, either with the Cary 17 or the Fourier Transform Spectrometer scanning at higher wavelengths.

The Van der Pauw (14) method was used to measure electrical resistivities and Hall voltages. Room temperature Seebeck coefficients were measured by applying a thermal gradient to the sample and recording the resulting voltage drop. The room temperature resistivity of NiP_2 crystals selected from two different batches prepared in the same manner (as described in the experimental section) ranged from 0.42 Ω-cm to 0.09 Ω-cm. Figure 5 shows the electrical resistivity of one of these crystals measured as a function of $10^3/T$ from 35°K to 560°K. The resistivity of NiP_2 decreases with increasing temperature between 35°K and 100°K. This behavior is characteristic of the extrinsic resistivity of a semiconductor at low temperature and is due to the promotion of electrons from impurity levels to the conduction band. The value of the activation energy of the impurity levels calculated from this extrinsic region is 0.002 eV. Between T = 100°K and T = 320°K, the slope of the resistivity plot changes sign. All the electrons from the impurity levels have been promoted to the conduction band and although the number of carriers remains essentially constant, their mobility decreases because of increased scattering by lattice vibrations, thus causing a rise in the value of the resistivity. Above T = 320°K, the thermal energy promotes an increased number of electrons from the valence to the conduction band. This causes a rapid decrease in the resistivity with increasing temperature and represents the onset of the intrinsic region. From this intrinsic range, a lower bound of 0.3 eV was calculated for the thermal band gap. From Seebeck and Hall measurements, the sign of the majority

carriers was found to be negative. The number of majority carriers was calculated assuming a single band conduction model.

The temperature dependence of the resistivity of a flux grown crystal of CuP_2 is compared with the resistivity of a CuP_2 crystal grown by chemical vapor transport in the temperature range of 70°K - 570°K (Figure 6). As seen in this figure, the resistivity plots for both materials are nearly coincident. From the linear segment of each plot (70 - 220°K), the activation energy of impurity states in the extrinsic region was calculated to be 0.03 eV *for both samples*. The exhaustion region occurs above 220°K for these samples. Contrary to the NiP_2 case, the onset of the intrinsic region could not be reached in the temperature range studied. This reflects the fact that the band gap of CuP_2 is approximately twice that of NiP_2. The room temperature resistivity values for four different CuP_2 samples are listed in Table III. P-type *conduction* was determined from Seebeck and Hall measurements.

Figure 7 shows that the resistivity of RhP_3 increases with increasing temperature over the whole temperature range studied (4 to 300°K).

CONCLUSION

From this study of single crystals grown from a tin flux, NiP_2 was ascertained to be a diamagnetic n-type semiconductor with a band gap of 0.7 eV. The observed diamagnetic behavior of NiP_2 is consistent with the presence of low spin d^8 configuration for the nickel atom.

The magnetic, optical and electrical properties of single crystals of CuP_2 grown from a tin flux were studied and found to be very similar to those of single crystals of CuP_2 grown by the chemical vapor transport technique. This similarity indicates that the tin did not substitute chemically into the CuP_2 structure but rather occurred as inclusions, as observed experimentally on flux grown crystals.

The negative and temperature independent magnetic susceptibility of RhP_3 indicates the presence of low spin state d^6 rhodium in this compound. Hall, Seebeck and resistivity measurements indicate p-type metallic conduction.

Table IV summarizes the transport properties of the different phases investigated.

ACKNOWLEDGEMENT

REFERENCES

1. W. Blitz and M. Heimbrecht, Z. Anorg. Allg. Chem. 237, 132 (1938).

2. A. Wilson, in Mellor's Comprehensive Treatise on Inorganic and Theoretical Chemistry , Vol. 8, Supplement 3.

3. A. Finley, D. Schleich, J. Ackermann, S. Soled, and A. Wold, Mat. Res. Bull., 9, 1655 (1974).

4. J. Ackermann and A. Wold, J. Phys. Chem. Sol., (1977) to be published.

5. I. Oftedal, Z. Krist., 66, 517 (1928).

6. D. Elwell and H. J. Scheel, Crystal Growth from High Temperature Solutions , Academic Press, London, 1975.

7. N. A. Goryunova, V. M. Orlov, V. I. Sokolova, G. P. Shpenkov, and E. V. Tsvetkova, Phys. Stat. Sol., 3, 75 (1970).

8. E. B. Sandell, Colorimetric Determination of Traces of Metals, 2nd Edition, Vol. III, pp. 470, Interscience, N.Y., N.Y. (1950).

9. O. Olofsson, Acta Chem. Scand., 19, 229 (1965).

10. E. Larsson, Ark. Kemi, 23, 335 (1964).

11. S. Rundqvist and N. O. Ersson, Ark. Kemi., 30, 103 (1968).

12. R. L. Adams, Ph.D. Thesis, Brown University, (1973).

13. B. Morris and A. Wold, Rev. Sci. Instrum., 39, 1937 (1968).

14. L. J. van der Pauw, Philips Res. Repts., 13, 1 (1958).

TABLE I

EXPERIMENTAL GROWTH CONDITIONS AND RESULTS FOR

THE TIN FLUX METHOD

Nominal Composition	Metal/Phosphorus/Tin Molar Ratios	Results
CuP_2	1/2/5	good crystals
CuP_2	1/2/10	best crystals
CuP_2	1/2/20	good crystals
CuP_3	1/3/20	crystals of Cu_4SnP_{10}
CuP_4	1/4/20	crystals of Cu_4SnP_{10}
CuP_6	1/6/20	crystals of Cu_4SnP_{10}
NiP_2	1/2/20	good crystals
NiP_2	1/2/40	good crystals
NiP_5	1/5/40	crystals of NiP_2
RhP_3	1/3/40	best crystals
RhP_3	1/3/80	good crystals
RhP_6	1/6/10	crystals of RhP_3

Soaking temperature = 1150°C

Cooling rate = 5°C/hour

Duration = 1 week

TABLE II

CRYSTALLOGRAPHIC DATA AND DENSITIES FOR CuP_2, NiP_2 AND RhP_3

	Space Group	a_o(Å)	b_o(Å)	c_o(Å)	β(°)	d_{calc}(g/cm^3)	d_{obs}(g/cm^3)
CuP_2 (CVT)	$P2_1/c$	5.797	4.803	7.514	112.68	4.32	4.33
CuP_2 (Tin Flux)	$P2_1/c$	5.796	4.803	7.517	112.66	4.32	4.35
CuP_2[9]	$P2_1/c$	5.802	4.807	7.525	112.68		
NiP_2	$C2/c$	6.363	5.615	6.072	126.23	4.57	4.58
NiP_2[10]	$C2/c$ or Cc	6.366	5.615	6.072	126.22		
RhP_3	$Im3$	7.991				5.09	5.07
RhP_3[11]	$Im3$	7.9951					

TABLE III

ROOM TEMPERATURE RESISTIVITY VALUES

FOR DIFFERENT CuP_2 SAMPLES

GROWTH TECHNIQUE	$\rho(\Omega\text{-cm})$
CVT	0.103
Tin flux (1/2/5)	0.139
Tin flux (1/2/10)	0.126
Tin flux (1/2/20)	0.145

TABLE IV

TRANSPORT PROPERTIES OF CuP_2, NiP_2 AND RhP_3

	CuP_2 (chemical vapor)	CuP_2 (tin flux)	NiP_2	RhP_3
$\rho_{77°K}$ (Ω-cm)	0.97	1.14	0.29	4.87×10^{-5}
$\rho_{290°K}$ (Ω-cm)	0.106	0.126	0.39	14.03×10^{-5}
number of carriers (77°K)	1.0×10^{16}	0.6×10^{16}	7.3×10^{17}	0.37×10^{20}
number of carriers (290°K)	6.6×10^{17}	4.3×10^{17}	8.7×10^{17}	0.6×10^{20}
Sign of carriers				
Hall	+	+	−	+
Seebeck	+	+	−	+
Seebeck Coef. (μV/°C)		692	392	32
Activation energy of impurity levels (eV)	0.03	0.03	0.002	
Optical absorption edge (eV)	1.55	1.51	0.73	

FIGURE CAPTION SHEET

Fig. 1 - CuP_2 Structure Projected on (010).

Fig. 2 - NiP_2 Structure Projected on (10$\bar{1}$).

Fig. 3 - Skutterudite Structure.

Fig. 4 - Optical Absorption Spectrum for CuP_2 and NiP_2.

Fig. 5 - Resistivity vs. $10^3/T$ for NiP_2.

Fig. 6 - Resistivity vs. $10^3/T$ for CuP_2.
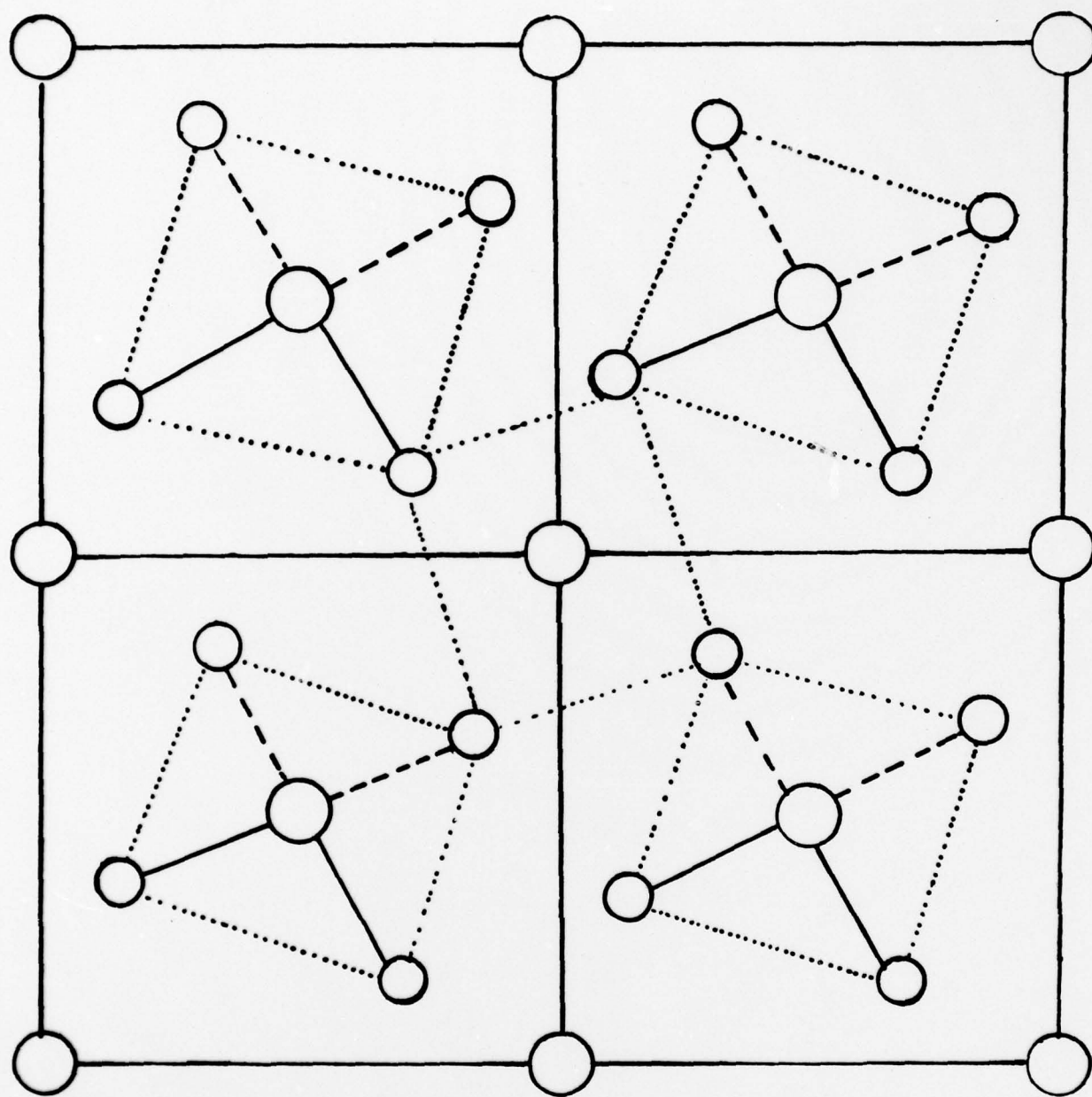
Fig. 7 - Resistivity vs. T for RhP_3.
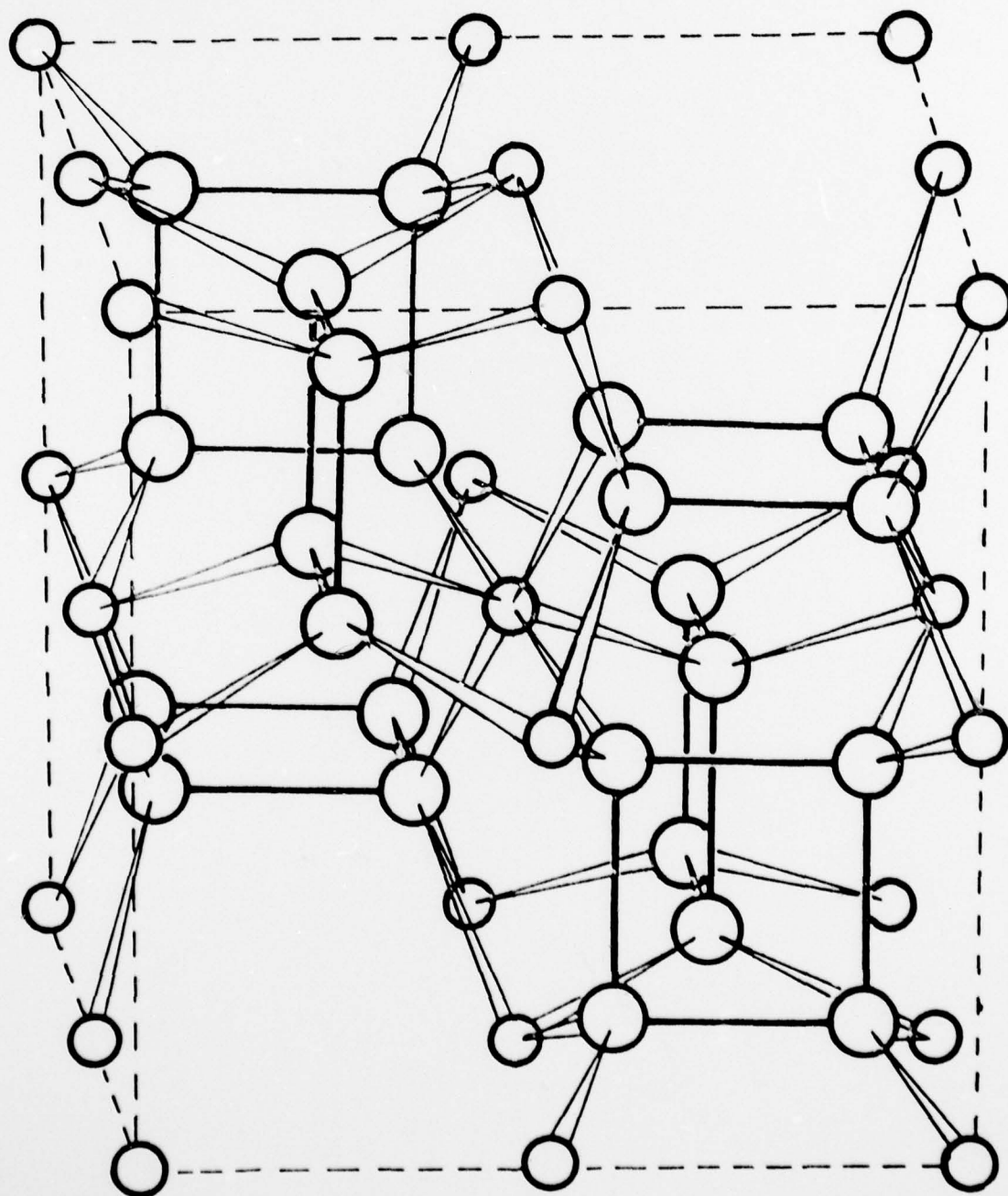
FIG 1
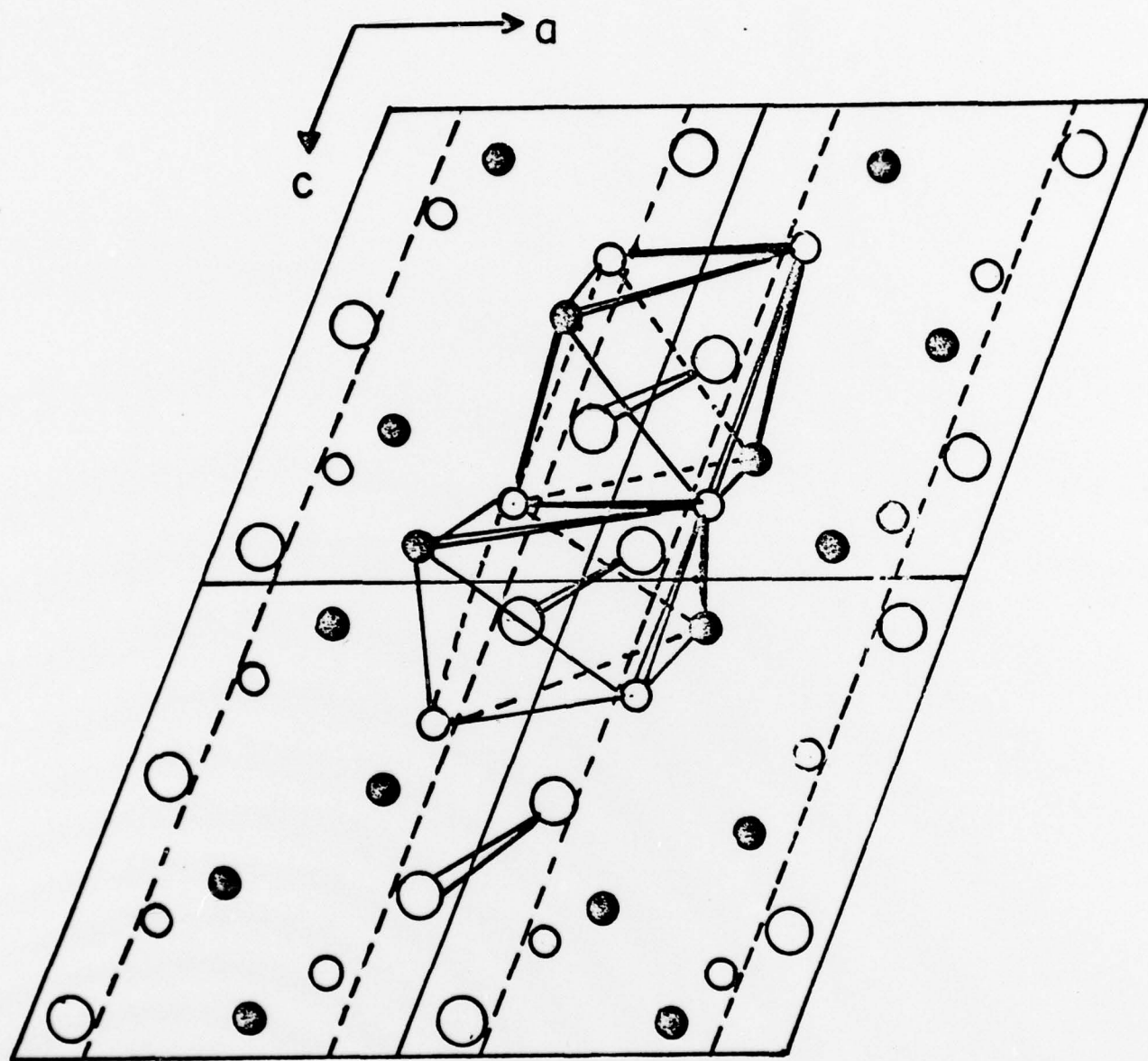
○ Cu   ○ P_i

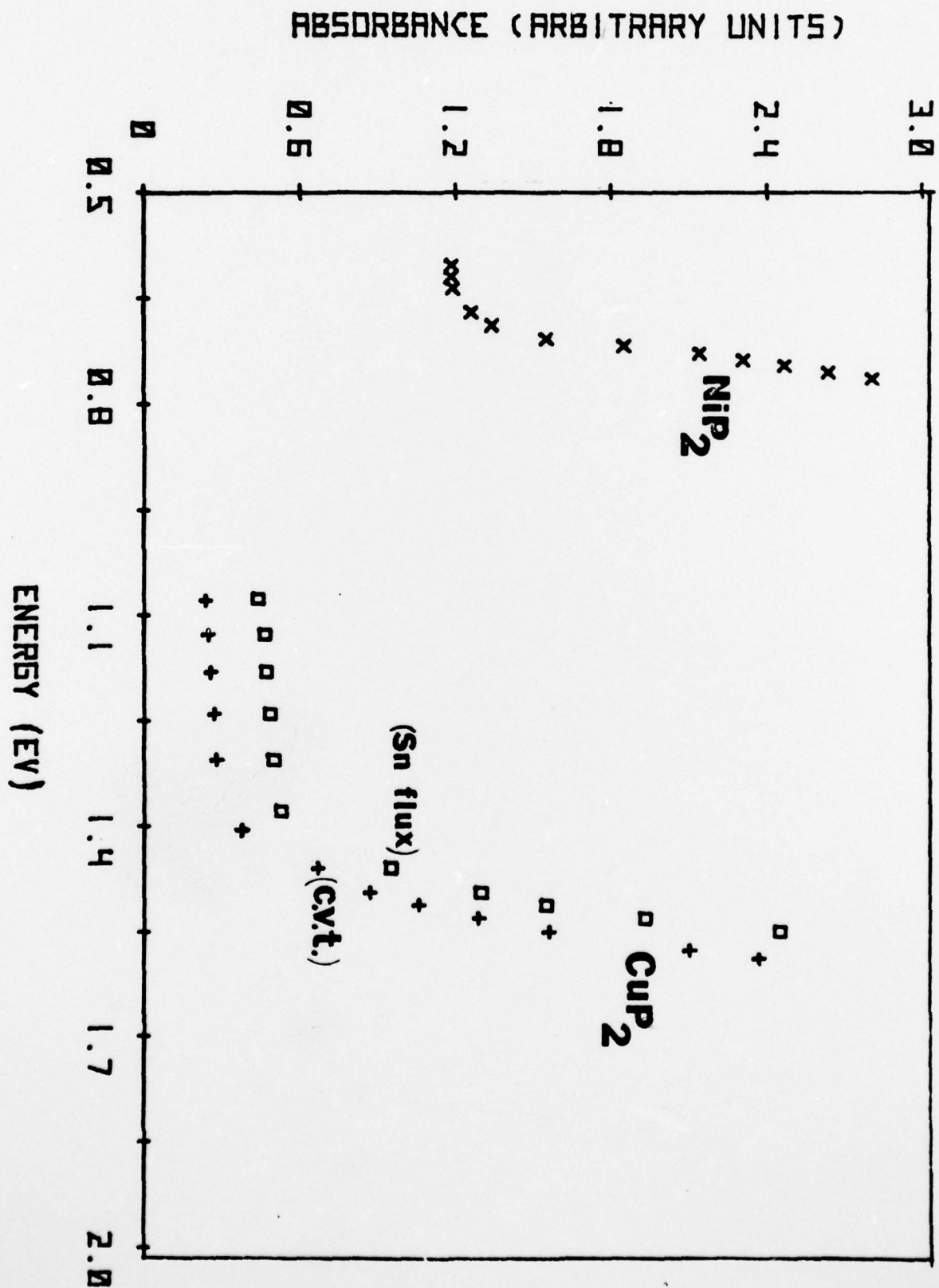● P_{ii}
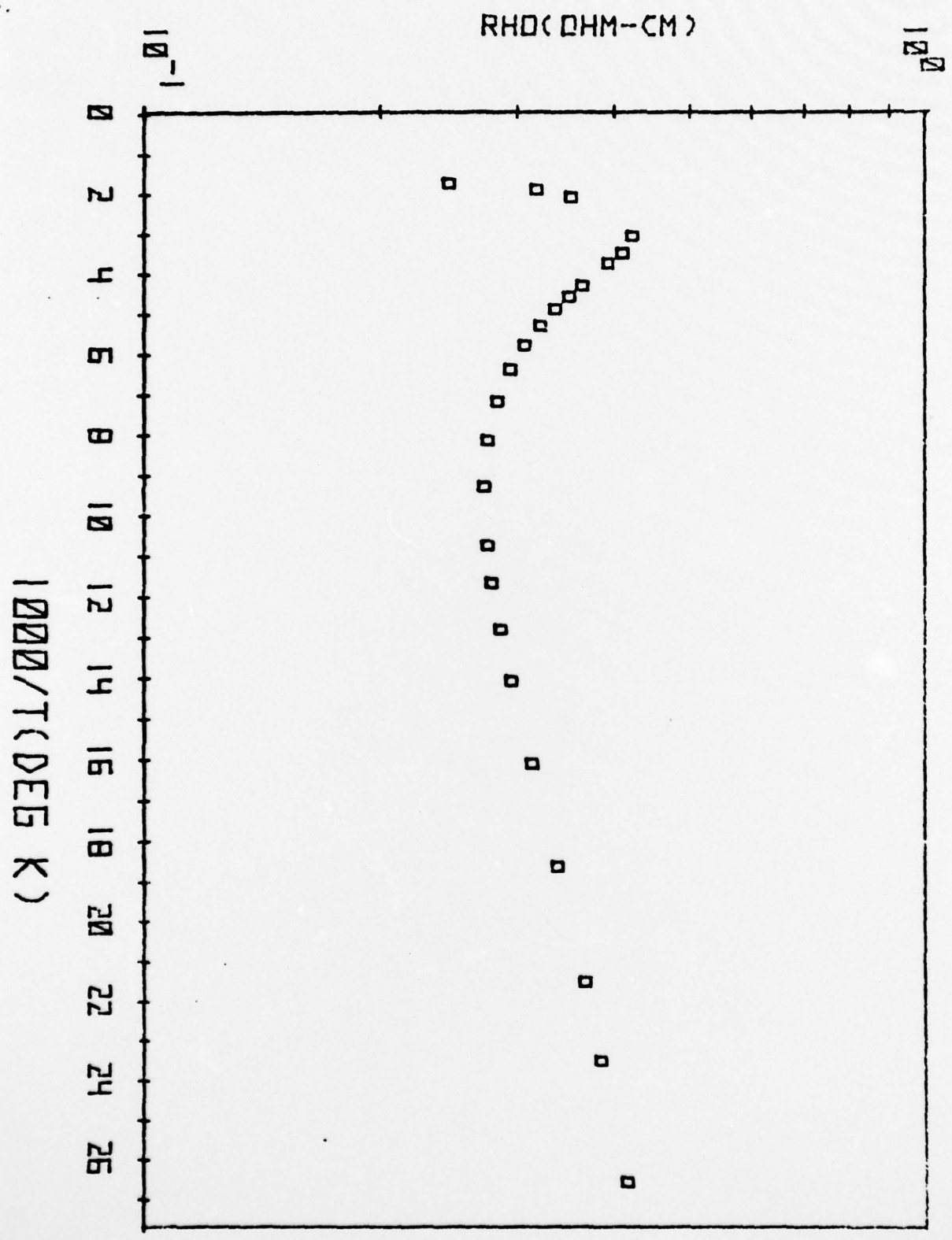
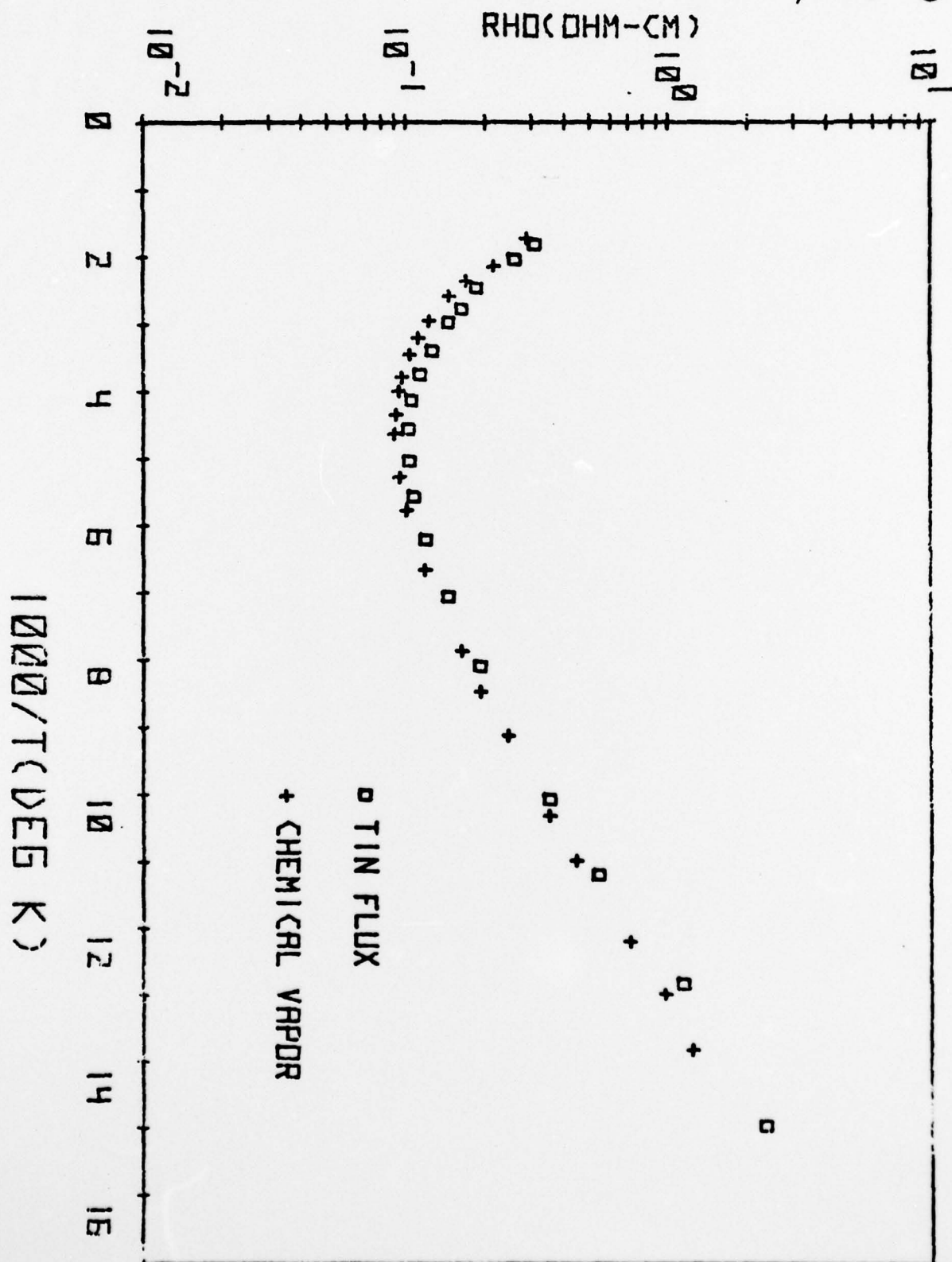FIG 2

Ni

P

FIG 3

Rh ○　x ○

Skutterudite

FIG 4

FIG 5

FIG 6

FIG 7